

Geometric and electronic properties of two kinds of CrO₂ magnetic monolayers: D_{3d} and D_{2h} phases

Yang Zhang¹, Xianggong Bo¹, Jimeng Jing, Lixia Wang, Shiqian Qiao, Hong Wu, Yong Pu, Feng Li *

New Energy Technology Engineering Laboratory of Jiangsu Province & School of Science, Nanjing University of Posts and Telecommunications (NJUPT), Nanjing 210046, China

Author Information

Yang Zhang¹, Xianggong Bo¹ contributed equally to this work

Corresponding Author

Feng Li *:lifen@njupt.edu.cn

Abstract

Due to the high magnetic coupling strength between the Cr elements, the bulk phase CrO₂ is one of several ferromagnetic oxides known to have the highest Curie temperature. When the dimensionality of the material is reduced from 3D to 2D, the 2D CrO₂ system material is expected to maintain a high Curie temperature. In this work, we predict two new phases of CrO₂ monolayer (D_{3d} and D_{2h}) by using first-principles calculations. We have found that the Curie temperature of 2D CrO₂ is much lower than that of its bulk phase, but still remains as high as 191K, which is comparable to that of Fe₂Cr₂Ge₆. In addition, 1L D_{3d}-CrO₂ is in the ferromagnetic state, while 1L D_{2h}-CrO₂ is in the antiferromagnetic state. Also, the different geometric structure affects its electrical properties: the 1L D_{3d}-CrO₂ is a half-metal while 1L D_{2h}-CrO₂ is a semiconductor. Our studies have shown that there is a wealth of electrical and magnetic properties in CrO₂.

Keywords: D_{2h}-CrO₂, D_{3d}-CrO₂, Geometric properties, electronic properties

Introduction

Bulk CrO₂ is one of several known ferromagnetic oxides, and is the ferromagnetic half-metal that has been experimentally confirmed^{[1][2][3][4]}. It has a rutile structure with Cr ions forming a tetragonal centroid lattice. Cr⁴⁺ has a closed shell Ar core and two additional 3d electrons. The Cr ions are in the center of the octahedra^[5]. The saturation magnetization at 10 K was reported to be 1.92 μ_B per Cr site^[6], which is close to the ideal value (2 μ_B) and is consistent with half-metallicity. It has a high Curie temperature, determined experimentally in the range of 385-400K^[7]. In a half-metallic ferromagnet, the conduction electrons should be completely spin polarized. This makes CrO₂ a good candidate for use as a spin injector and has sparked the revival of CrO₂ thin film growth techniques^[7] including the original high-pressure, thermal decomposition method as well as a chemical vapor deposition (CVD) technique discovered in the late 1970s^[8].

In the past two decades, with the discovery of graphene^[9], the attention of two-dimensional materials has gradually increased. Two dimensional materials have more advantages in spin electronic devices because of their simple

structure and easy magnetic control. In 2017, the first intrinsic ferromagnetic two-dimensional CrI₃ and CrGeTe₃ were successfully fabricated for the first time^{[10][11]}, bringing the study of ferromagnetism from 3D down to 2D. When materials are transformed from bulk into their two-dimensional (2D) forms, new physical phenomena may appear. Unfortunately, there are few reports on the 2D structure of CrO₂ till now. The past studies on half-metal magnets mostly focused on the bulk systems. What necessary to develop low-dimensional half-metal materials is spintronic devices with the demand of small size and high capacity, especially two-dimensional (2D) nanosheets or monolayer materials due to the simple synthesis, ultra-thin thickness, and adjustable electronic structure^[12].

In this work, we predicted two lowest-energy structures of CrO₂ monolayer, namely 1L D_{3d}-CrO₂ and D_{2h}-CrO₂^{[13][14]}. They all have high geometric stability, while having significantly different electronic and magnetic properties. The D_{3d}-CrO₂ has the lowest energy, which is 178.16 meV / cell than that of D_{2h}-CrO₂. The D_{3d}-CrO₂ is half-metal ferromagnetic while the D_{2h}-CrO₂ is an antiferromagnetic semicon-

ductor. The both 1L D_{3d} -CrO₂ and D_{2h} -CrO₂ could be prepared by advanced chemical vapor deposition method^{[15][16]}.

Methods

Our first-principles calculations were based on density functional theory (DFT) implemented in the *Vienna Ab initio Simulation Package* (VASP)^[17]. Generalized gradient approximation (GGA) for exchange-correlation functional given by *Perdew-Burke-Ernzerhof* (PBE)^[18] was used. The effective Hubbard $U_{\text{eff}} = 2.6$ eV was added according to *Dudarev's* method for the Cr- d orbitals^{[19][20][21]}. The projector augmented wave (PAW)^[22] method was used to treat the core electrons. The plane wave cutoff energy was set to be 500 eV. The first Brillouin zone was sampled by using a Γ -centered $20 \times 20 \times 1$ Monkhorst-Pack^[23] grid for D_{3d} CrO₂ and $10 \times 16 \times 1$ Monkhorst-Pack grid for D_{2h} CrO₂. The lattice geometries and atomic positions were fully relaxed until force and the energy were converged to 0.01 eV \AA^{-1} and 10^{-6} eV, respectively. Van der Waals interaction (vdW) correlation is considered by using the semi-empirical dispersion-corrected density functional theory (DFT-D3) force-field approach^[24]. A vacuum space of 20 \AA along the z direction was adopted to model the 2D system. The spin-orbit coupling (SOC) was included in the electronic self-consistent calculations. The phonon dispersion relations was calculated by employing the density-functional perturbation theory (DFPT) and PHONOPY^[25]. The Monte Carlo simulation with Wolff algorithm^[26] half-metal based on classical Heisenberg model is used to describe the thermal dynamics of magnetism in equilibrium states^{[26][27]}. All the renormalization group Monte Carlo algorithm^[28] half-metals were implemented in the open source project MCSOLVER^[29].

Results and discussion

1 D_{3d} CrO₂ monolayer

We carefully check energy orders of ferromagnetic states (FM) and antiferromagnetic states (AFM) for the two phases of CrO₂. For D_{3d} CrO₂, the $4 \times 4 \times 1$ Cr supercells for ferromagnetic state and two antiferromagnetic states are considered to calculate the relative energy (Fig. 1c). The relative energy for these magnetic states are 0, 44.166 and 71.085 meV / unit cell for supercells, respectively. The FM

state has the lowest Energy. Therefore, the ground state of D_{3d} CrO₂ is ferromagnetic.

The structure of CrO₂ monolayer with D_{3d} symmetry is shown in Fig. 1a. For D_{3d} CrO₂, the equilibrium lattice constant a and b are 2.92 \AA . A Cr atom is surrounded by six O atoms each of them bonded to three Cr atoms. The bond length between Cr and O atom is 1.94 \AA . The total magnetic moment is 2 μ_B / unit cell. The majority of the total magnetic moment comes from the Cr atoms, while the O atoms have a small magnetic moment of only 0.18 μ_B . The magnetic calculations show that the monolayer behaves as a ferromagnetic half-metal, as shown in Fig. 1b, which is provide a new possibility to implement the intrinsic half-metallicity without any artificial modification. The spin-up channels of D_{3d} CrO₂ possess a very large band gap, whereas the spin-down ones do not show any gap. Electrons around the Fermi level are contributed by Cr- d and O- p orbitals. Therefore, the electronic structure has an intrinsic half-metallicity without any artificial modification.

Next, we explore the magnetic behavior under finite temperatures. Here we use the Heisenberg model to describe the magnetic behavior of these systems. The spin Hamiltonian can be written as

$$H = - \sum_{ij} J_{ij} S_i \cdot S_j \quad (1)$$

where J is the exchange interaction parameter, $S = 2/2$ for Cr.

Here we considered one typical coupling channel for D_{3d} CrO₂ (Fig. 2a). In order to calculate the energy difference between AFM and FM more accurately, we used $2 \times 2 \times 1$ supercells to calculate the exchange coupling strength (Fig. 2b). The energy difference was calculated to be 245.35 meV per $2 \times 2 \times 1$ supercell.

According to equation 1, the energies arising from spin exchange for FM and AFM can be written as

$$E_{FM} = E_0 - 12JS^2 \quad (2)$$

$$E_{AFM} = E_0 + 4JS^2 \quad (3)$$

The magnetic coupling was calculated to be 15.33 meV. Positive values represent FM exchange interactions. Therefore, the nearest neighbour exchange interaction is ferromagnetic.

Then by classical Metropolis MC simulations (Fig. 2c), the T_c of D_{3d} CrO₂ is 191 K.

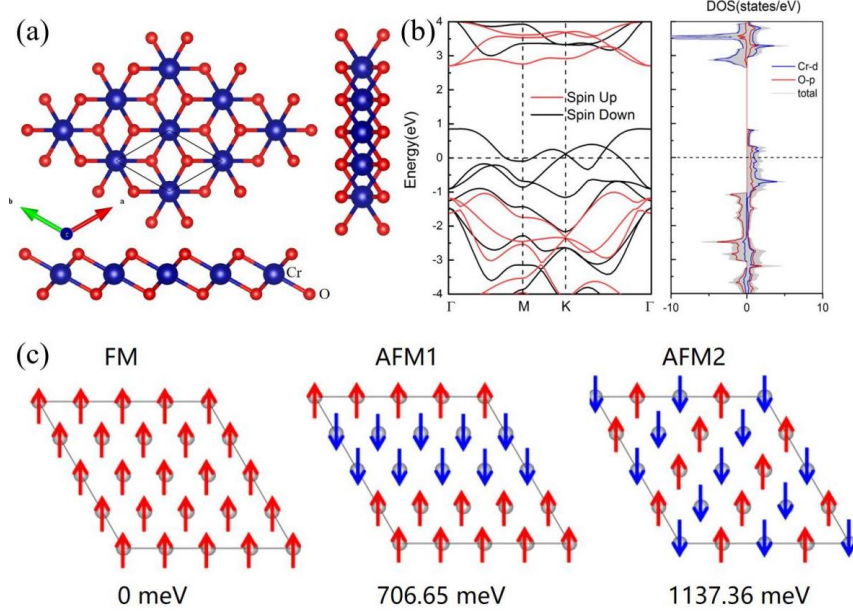


Fig. 1 (a) Structure of D_{3d} CrO_2 with top, front and right view. (b) Electronic band structure and density of state of D_{3d} CrO_2 . (c) The ferromagnetic state and two antiferromagnetic states of D_{3d} CrO_2 in $4 \times 4 \times 1$ Cr supercells. Including their relative energy.

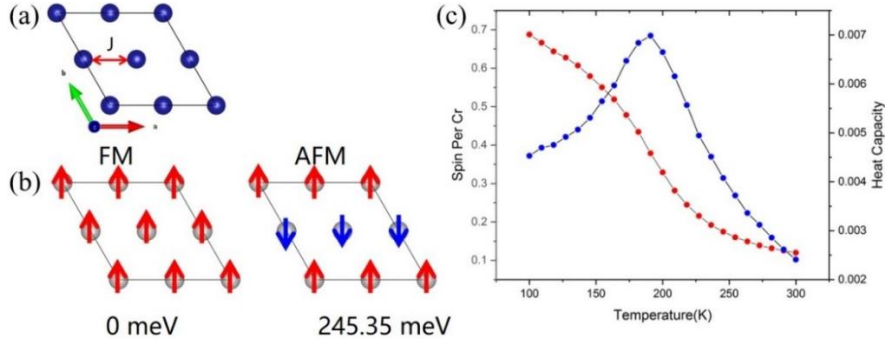


Fig. 2 (a) One classic exchange strength J shown in a $2 \times 2 \times 1$ Cr supercell. For simplicity, O atoms are removed. (b) The ferromagnetic state and antiferromagnetic state of D_{3d} CrO_2 in $2 \times 2 \times 1$ Cr supercells. Including their relative energy. (c) MC simulations of T_c of D_{3d} CrO_2 monolayer.

II D_{2h} CrO_2 monolayer

Then we discuss the CrO_2 monolayer with D_{2h} symmetry. For D_{2h} CrO_2 , the $2 \times 2 \times 1$ Cr supercells for ferromagnetic state and three antiferromagnetic states are considered to calculate the relative energy (Fig. 3c). The relative energy for these magnetic states are 0, 557.82, 726.37 and 870.32 meV for supercells, respectively. The AFM1 state has the lowest Energy. Therefore, the ground state of D_{2h} CrO_2 is antiferromagnetic.

The structure of this phase is shown in Fig. 3a. For D_{2h} CrO_2 , the equilibrium lattice constant a and b are 5.01 and 2.90 Å, respectively. In a CrO_2 unit, there are two typical chemical bond lengths. Four bonds are 1.95 Å and the rest two are 1.93 Å. The magnetic calculations show that the monolayer behaves as an antiferroma-

gnetic semiconductor, as shown in Fig. 3b. D_{2h} CrO_2 is semiconducting with sizable electronic energy gap (~ 1.00 eV). The edges of the valence bands are coming from the d orbitals of Cr atoms and p orbitals of O atoms, while the conduction band edges are mainly coming from Cr-d orbitals and partly from the O-p orbitals. For D_{2h} CrO_2 , the two Cr atoms have three typical coupling channels whose strengths are labelled as J_1 , J_2 and J_3 (Fig. 3a). According to equation 1, the energies arising from spin exchange for FM, AFM1, AFM2 and AFM3 can be written as

$$E_{FM} = E_0 - 8J_1S^2 - 16J_2S^2 - 8J_3S^2 \quad (4)$$

$$E_{AFM1} = E_0 + 8J_1S^2 - 8J_3S^2 \quad (5)$$

$$E_{AFM2} = E_0 - 8J_1S^2 + 8J_3S^2 \quad (6)$$

$$E_{AFM3} = E_0 - 8J_1S^2 + 16J_2S^2 - 8J_3S^2 \quad (7)$$

The magnetic coupling exhibits an anisotropy

since the obtained J_1 , J_2 and J_3 equal to -42.22, 10.21 and 0.52 meV. The nearest neighbour exchange interaction is antiferromagnetic, the

second neighboring and the third neighboring exchange parameters are ferromagnetic.

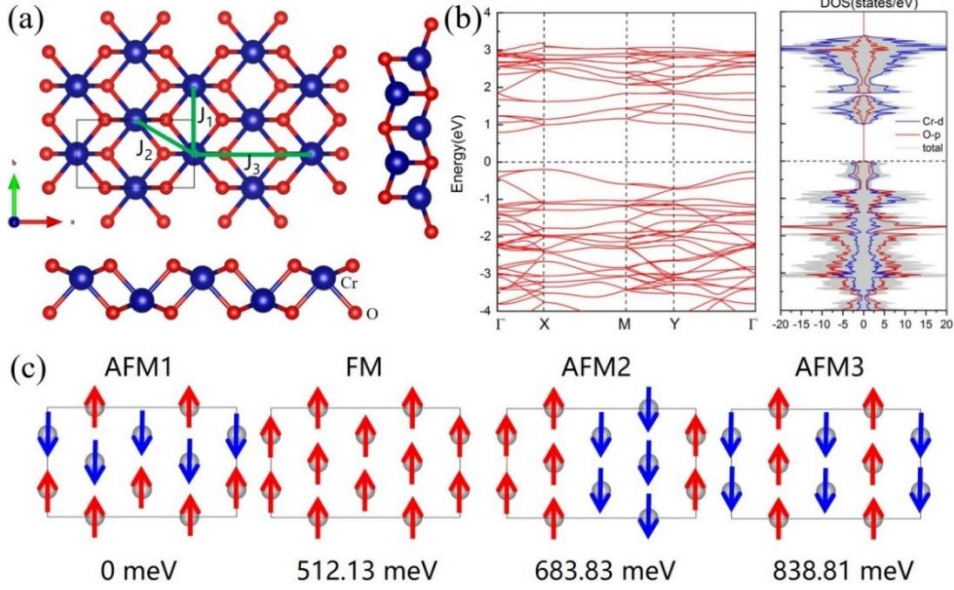


Fig. 3 (a) Structure of D_{2h} CrO_2 with top, front and right view. Including three classic exchange strength J_1 , J_2 and J_3 . (b) Electronic band structure and density of state of D_{2h} CrO_2 . (c) The ferromagnetic state and two antiferromagnetic states of D_{2h} CrO_2 in $2 \times 2 \times 1$ Cr supercells. Including their relative energy.

III Geometric Stability

To assess the low phases of CrO_2 is dynamically stable, we study its lattice dynamics by calculating the phonon dispersion. The result of D_{3d} is shown in Fig.4a. For monolayer CrO_2 , the phonon branches is positive in the whole Brillouin zone, so the absence of imaginary mode in the entire

Brillouin zone confirms that D_{3d} is dynamically stable. In Fig.4b we can find that one third of the spectral lines around Γ are below 0, which is negative. But it is very likely to be stable, maybe because the structural accuracy is not optimized enough, which is also encountered in some other 2D materials, and further improving the optimized accuracy or adding a little tensile strain can eliminate this virtual frequency.

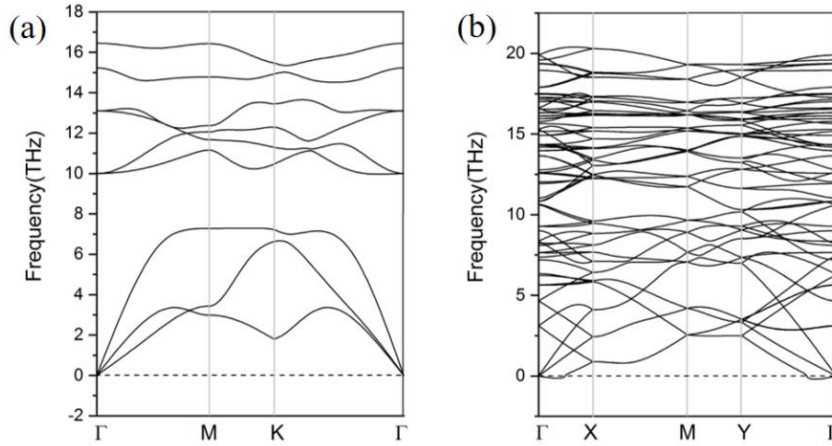


Fig. 4 The phonon spectrum calculations for (a) D_{3d} and (b) D_{2h} CrO_2 .

Conclusion

In summary, based on first-principles calculations, we predict two phases of CrO₂ monolayer (D_{3d} and D_{2h}). Our results indicate that the ground state of D_{3d} CrO₂ is FM with estimated T_c of 191 K. And it is an intrinsic half-metal with 100 % spin polarization, which can be applied in high-quality magnetic recording medium. In contrast, the D_{2h} -CrO₂ is an anti-ferromagnetic semiconductor, which renders 2D CrO₂ sheet a very promising candidate for AFM spintronics in nanoscale. Our calculations suggest that the two phases of CrO₂ can provide a great platform for building spintronic devices and can stimulate relevant experiments.

Reference

- [1] Schwarz, CrO₂ predicted as a half-metallic ferromagnet, 16 (1986) 211-216. DOI:10.1088/0305-4608/16/9/002
- [2] H.Y. Hwang, S. Cheong, Enhanced intergrain tunneling magnetoresistance in half-metallic CrO₂ films, Science, 278 (1997) 1607-1609. DOI:10.1126/science.278.5343.1607
- [3] Y. Ji, G.J. Strijkers, F.Y. Yang, C.L. Chien, J.M. Byers, A. Anguelouch, G. Xiao, A. Gupta, Determination of the spin polarization of half-metallic CrO₂ by point contact Andreev reflection, Phys Rev Lett, 86 (2001) 5585-5588. DOI:10.1103/physrevlett.86.5585
- [4] I., I., Mazin, D., Singh, Claudia, Ambrosch-Draxl, Transport, optical, and electronic properties of the half-metal CrO₂, Physical Review B, 85 (1999) 6220-6222. DOI:10.1063/1.370227
- [5] L. Chioncel, H. Allmaier, E. Arrighoni, A. Yamasaki, A.I. Lichtenstein, Half-Metallic Ferromagnetism and the spin polarization in CrO₂, Physical review. B, Condensed matter, 75 (2007) 1418-1428. DOI:10.1103/PhysRevB.75.140406
- [6] Y. Moritomo, R. Yamamoto, A. Nakamura, Electronic structure of half-metallic CrO₂ as investigated by optical spectroscopy, Phys.rev.b, 61 (2000) 5062-5064. DOI:10.1103/PhysRevB.61.R5062
- [7] S.M. Watts, S. Wirth, S.V. Molnár, A. Barry, J. Coey, Evidence for two-band magnetotransport in half-metallic chromium dioxide, Physical Review B, 61 (2000) 9621-9628. DOI:10.1103/PhysRevB.61.9621
- [8] S. Ishibashi, T. Namikawa, M. Satou, Epitaxial Growth of CrO₂ on Sapphire in Air, Japanese Journal of Applied Physics, 17 (1978) 249-250. DOI:10.1143/JJAP.17.249/meta
- [9] K.S. Novoselov, A.K. Geim, S.V. Morozov, D. Jiang, Y. Zhang, S.V. Dubonos, I.V. Grigorieva, A.A. Firsov, Electric field effect in atomically thin carbon films, Science, 306 (2004) 666-669. DOI:10.1126/science.1102896
- [10] B. Huang, G. Clark, E. Navarro-Moratalla, D.R. Klein, R. Cheng, K.L. Seyler, D. Zhong, E. Schmidgall, M.A. McGuire, D.H. Cobden, W. Yao, D. Xiao, P. Jarillo-Herrero, X. Xu, Layer-dependent ferromagnetism in a van der Waals crystal down to the monolayer limit, Nature, 546 (2017) 270-273. https://www.nature.com/articles/nature22391
- [11] C. Gong, L. Li, Z. Li, H. Ji, A. Stern, Y. Xia, T. Cao, W. Bao, C. Wang, Y. Wang, Z.Q. Qiu, R.J. Cava, S.G. Louie, J. Xia, X. Zhang, Discovery of intrinsic ferromagnetism in two-dimensional van der Waals crystals, Nature, 546 (2017) 265-269. https://www.nature.com/articles/nature22060
- [12] Y. Feng, X. Wu, J. Han, G. Gao, Robust half-metallicities and perfect spin transport properties in 2D transition metal dichlorides, Journal of Materials Chemistry C, 6 (2018) 4087-4094. https://doi.org/10.1039/C8TC00443A
- [13] B. Zhang, J. Sun, J. Leng, C. Zhang, J. Wang, Tunable two dimensional ferromagnetic topological half-metal CrO₂ by electronic correction and spin direction, Applied Physics Letters, 117 (2020) 222407. https://doi.org/10.1063/5.0031443
- [14] X. Deng, Z. Li, Intrinsic ultra-wide completely spin-polarized state realized in a new CrO₂ monolayer, Physical Chemistry Chemical Physics, (2020) 1-4. https://doi.org/10.1039/D0CP02627A
- [15] M. Xu, T. Liang, M. Shi, H. Chen, Graphene-like two-dimensional materials, Chem Rev, 113 (2013) 3766-3798. https://pubs.acs.org/doi/10.1021/cr300263a
- [16] T. Gould, S. Lebègue, T. Björkman, J.F. Dobson, Chapter One - 2D Structures Beyond Graphene: The Brave New World of Layered Materials and How Computers Can Help Discover Them, Semiconductors and semimetals, 95 (2016), 1-33. https://doi.org/10.1016/bs.semsem.2016.04.001
- [17] G. Kresse, J. Hafner, Ab initio molecular dynamics for liquid metals, Phys Rev B Condens Matter, 47 (1993) 558-561. https://doi.org/10.1016/0022-3093(93)00355-X
- [18] J.P. Perdew, K. Burke, M. Ernzerhof, Generalized Gradient Approximation Made Simple, Physical Review Letters, 77 (1996) 3865-3868. https://journals.aps.org/prl/abstract/10.1103/PhysRevLett.77.3865
- [19] X. Li, J. Yang, CrXTe₃ (X = Si, Ge) nanosheets: two dimensional intrinsic ferromagnetic semiconductors, Journal of Materials Chemistry C, 2 (2014) 7071-7076. https://doi.org/10.1039/C4TC01193G
- [20] B. Deng, X.Q. Shi, L. Chen, S.Y. Tong, Preserving half-metallic surface states in CrO₂: Insights into surface reconstruction rules, Physical Review B, 97 (2018) 165404. DOI:https://doi.org/10.1103/PhysRevB.97.165404
- [21] L. Chioncel, H. Allmaier, E. Arrighoni, A. Yamasaki, M. Daghofer, M.I. Katsnelson, A.I. Lichtenstein, Half-metallic ferromagnetism and spin polarization in CrO₂, Physical Review B, 75 (2007) 140406. https://journals.aps.org/prb/abstract/10.1103/PhysRevB.75.140406
- [22] P.E. Blochl, Projector augmented-wave method, Phys Rev B Condens Matter, 50 (1994) 17953-17979. https://journals.aps.org/prb/abstract/10.1103/PhysRevB.50.17953
- [23] H.J. Monkhorst, J.D. Pack, Special points for Brillouin-zone integrations, Physical Review B, 13 (1976) 5188-5192. https://doi.org/10.1103/PhysRevB.13.5188
- [24] S. Grimme, J. Antony, S. Ehrlich, H. Krieg, A consistent and accurate ab initio parametrization of density functional dispersion correction (DFT-D) for the 94 elements H-Pu, J Chem Phys, 132 (2010) 154104. https://doi.org/10.1063/1.3382344
- [25] A. Togo, I. Tanaka, First principles phonon calculations in materials science, Scripta Materialia, 108 (2015) 1-5. https://doi.org/10.1016/j.scriptamat.2015.07.021
- [26] M. Kan, S. Adhikari, Q. Sun, Ferromagnetism in MnX₂ (X = S, Se) monolayers, Phys Chem Chem Phys, 16 (2014) 4990-4994. https://doi.org/10.1039/C3CP55146F
- [27] M. Kan, J. Zhou, Q. Sun, Y. Kawazoe, P. Jena, The Intrinsic Ferromagnetism in a MnO₂ Monolayer, J Phys Chem Lett, 4 (2013) 3382-3386. https://doi.org/10.1039/C3CP55146F
- [28] M. Lan, G. Xiang, Y. Nie, D. Yang, X. Zhang, The static and dynamic magnetic properties of monolayer iron dioxide and iron dichalcogenides, RSC Advances, 6 (2016) 31758-31761. https://doi.org/10.1039/C6RA03480B
- [29] Liu, L.; Zhang, X. A User Friendly and Efficient Tool Implementing Monte Carlo Simulations to Estimate Curie/Neel Temperature. https://github.com/golddoushi/mcsolver

